Response of RC High-rise building subjected to Blast Load

Mohanad Hatem Shadhar [1] , Abdul Aziz Abdul Samad [1], Noridah Mohamad [1], Akram Hatem [2]
[1] Faculty of Civil Engineering and Built Environment, Universiti Tun Hussein Onn Malaysia, 86400, Batu Pahat, Malaysia
[2] Al Kitab University College, Altun Kupri, Iraq

Abstract

Many countries have become victims of bomb blast attacks in the past few decades. Damage to resources, loss of life and social panic are components that need to be minimised if the threat of terrorist attacks cannot be halted. Also, attacks on important public buildings reflect the very need for the consideration of blast effects in the design. These impacts are dynamic in nature. To make structures safe against these blast effects, new concepts like blast resistant designs are gaining huge interest in present studies. Evaluation of structures and structural designs which are subjected to blast load plays one of the most important criteria. This present study is conducted to assess the effects of blast loads on high-rise structures which consist of three types of structures, namely, RC shear wall, RC frame and masonry structures. A finite element package ETABS was used for the analysis. The dynamic behaviour of high-rise RC structures were taken into consideration for they were subjected to an impact loads of 10 kN weapon charge. The effects of blast load on the structures were studied with varying distances from the point of explosion. Structures having different characteristics were subjected to blast overpressure at distances of 50m, 70m, 90m, 110m and 150m. The minimum distance at which the structure was safe against the blast force were found in the three types of the structures.

Keywords: Blast load, Explosion, RC structures, Radiation, masonry wall, shear wall

1. Introduction

A blast loading is characterised as a quick chemical reaction that happens in a few milliseconds, resulting in rapid release of energy and hot gases into the surrounding atmosphere. This causes a high generation of temperature and pressure [1]. During the blast loading, the hot gases that are generated occupy the surrounding space, resulting in a propagation wave through space which is transmitted either spherically or hem-spherically through the surrounding medium[2] [3] and [4]. The blast is determined by height, weight and temperature. Amid the blast, hot gases that are produced envelope the encompassing space, which comes about in a wave of proliferation through space which is transmitted roundly or fix-roundly through an encompassing medium. Unlike earthquake forces, blast pressure acts for a significantly shorter period of time on a structure[5]. Hence, effects of material strain rate becomes vital and should be be taken into account to assess the performance of connections for shorter duration loads i.e. blast loads [6]. This high impulsive load generally acts non-uniformly on the structure i.e. the aberration of load extent transversely to the face of the structure and greatly reduces the amplitudes of the blast pressure on the sides and back ends of the structure far from the explosion point.

Supersonic explosions however, are formed by extremely high explosives known as detonations and travel by means of supersonic shock waves [7] [8] . When the energy is released rapidly, a waveform of pressure within the surrounding space is created as a shock front [9]. However, the accumulation of hot gases occur because of the explosion. This causes a generation of high waves of pressure in the medium. These waves propagate with the same speed as sound at a high degree of temperature of 3000° to 4000° [3]. The absolute maximum pressure over and above the atmospheric pressure that occurs in the shock wave is called a maximum or peak value of overpressure [10]. Taking after the shock wave, overpressure decreases to about one-half of the greatest overpressure and holds on exceptionally at the central zone of the blast [11] [12] . This is the phase in which pressure due to explosion is greater.

Explosions can be classified into three types based on its reaction; physical, chemical and nuclear explosion. Physical explosion is a release of energy from a dangerous explosion of compressed gas cylinders or a combination of two liquids at extremely high temperatures [13]. A nuclear explosion can be defined as a sudden release of energy caused by redistribution of protons and neutrons inside the core resulting from the formation of atomic nuclei [14]. Whereas chemical explosion is caused by the release of energy of high rate oxidation of hydrocarbon elements such as carbon and hydrogen atoms. Explosives must be inactive and stable to utilise them. Explosion is usually triggered rather than an unconstrained response. The explosion is a process of quick and enormous discharge of energy. The speed of the reaction demonstrates the usefulness of explosive materials that can be condensed, solid or liquid. After exploding they deteriorate, transmitting heat and producing gas. Explosive materials as per their physical state are classified as solids, liquids or gases. Solid explosives are basically high explosives for they have extreme blast impacts. They can also be classified based on their sensitivity to start as secondary or essential explosives.

When explosion happens, the blast's shock waves transfer with increasingly rapid overpressure to the front as shown in Figure 1. The pressure behind the structure's face may indeed drop below the normal atmospheric pressure within milliseconds.

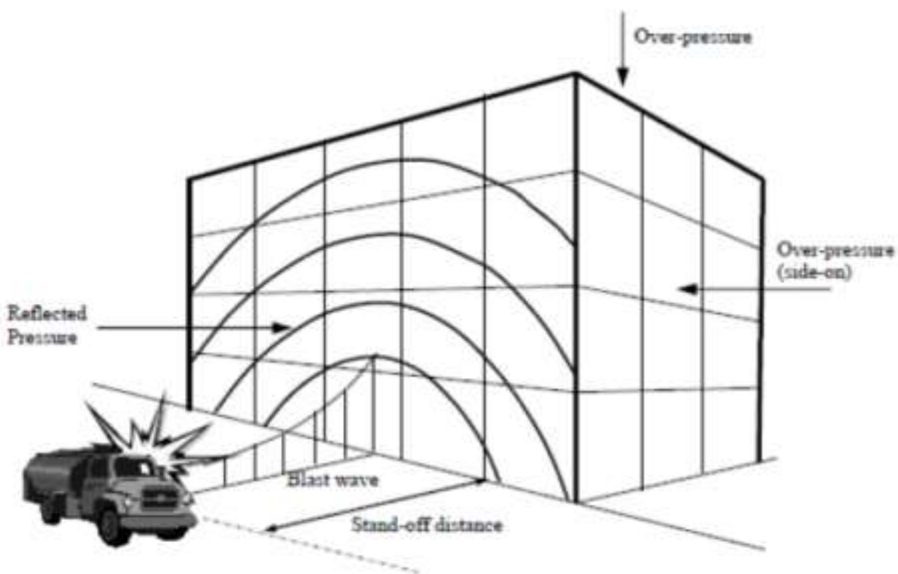

Figure 1. Effect of blast loads on a building

The minimum guaranteed distance between the blast source and targeted structure in Figure 1 is called a stand-off distance [15]. This is the requirement in keeping the explosion as far as possible from the structure by increasing the stand-off distance between the source of the blast and the target. This helps to minimise the damage where the size of the bomb does not matter in cases of congested areas where there is no provision for stand-off distance, bollards, trees or street furniture to provide as obstacles.

As the stand-off distance rises, the impact of overpressure on the shock front reduces considerably and its speed decreases to the speed of sound of an undisturbed surrounding medium. After a certain time, the overpressure within the shock front decreases to a value less than that of the medium and consequently it is called as a negative phase (Figure 2) [16].

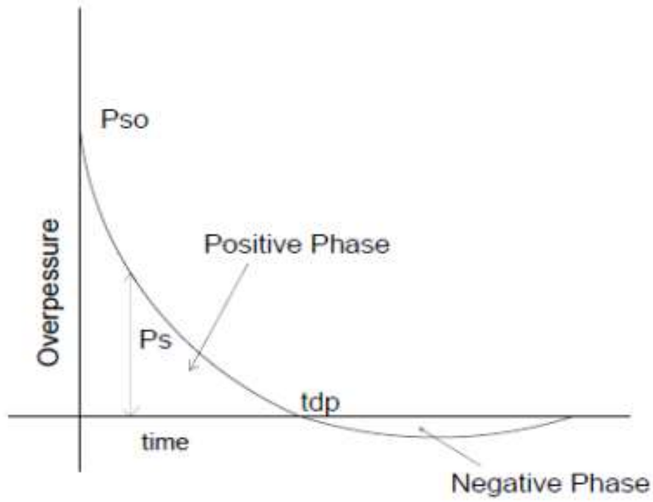

Figure 2. The variation of overpressure with distance at a given time from centre of explosion [Pso]

The overpressure with duration for a specific distance is illustrated in Figure 3 to demonstrate the time span of the positive phase and end time of the positive phase. In addition to overpressure, there is a parameter which is of equal importance known as dynamic pressure [Pdo]. Typically, it is in proportion to the air density rearward of the shock wave and square of the wind velocity. Variety of dynamic pressure with time is presented in Figure 3.

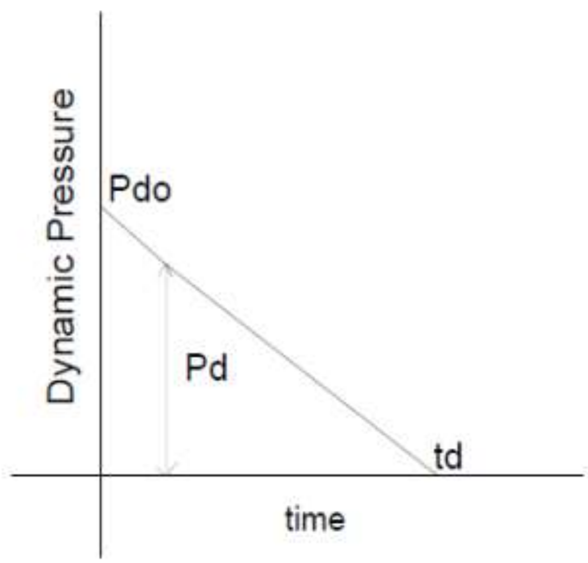

Figure.3 Variation of Dynamic pressure [Pdo]

The study assesses the performance of high-rise structures with the different cases as shown above and were subjected to a blast loading at stand-off distances of 30m, 50m, 70m, 90m, 110m and 150m. The modelling and analysis carried out uses the finite element models in FEM package ETABS. A 30-storey high structure with the following specification was considered for this study:

- RC Frame structural system.
- RC Frame structure with the shear wall at outer periphery (Shear wall structure).
- RC Frame structure with the masonry wall at outer periphery (Masonry wall structure).

 ISSN No : 1006-7930

2. Blast loads prediction

When explosion occurs, a rapid release of energy will form. From the point of explosion, a spherical shock wave will be generated and translated. This shock wave impinges on the target such as a building structure. Due to a reflection of the blast waves, high pressure is generated which causes force at the striking end. The blast load is non-uniformly distributed when the structure is subjected to blast load with a time lag. Air moving with high velocity after the shock front imparts drag force on the building. Therefore, three consequences play a significant role on the impact of blast load on a structure. They are namely, the effects of initial overpressure, reflection effects and drag force caused by dynamic pressure [17]

2.1 Peak value of Overpressure and Dynamic pressure

The variation of peak value of dynamic pressure, overpressure and time of positive phase of overpressure with a range or distance of the blast location are plotted in Figure 4 for weapon quantities ranging from 10 kN to 10^7 kN as documented in IS 4991.1968 [18]. The range values and the time durations for a distinct weapon quantity were obtained using the scaling laws below.

$$\frac{R_2}{R_2} = \left(\frac{Y_1}{Y_2}\right)^{\frac{1}{3}} \tag{1}$$

$$\frac{t_1}{t_2} = \left(\frac{Y_1}{Y_2}\right)^{\frac{1}{3}} \tag{2}$$

Equation 1 used for range scaling for a weapon quantity. Equation 2 used for time duration scaling for a weapon quantity. Where R1, R2 are the ranges to obtain the overpressure with yield of Y1 and Y2 respectively t1 and t2 are the time durations obtained at yield of Y1 and Y2 respectively.

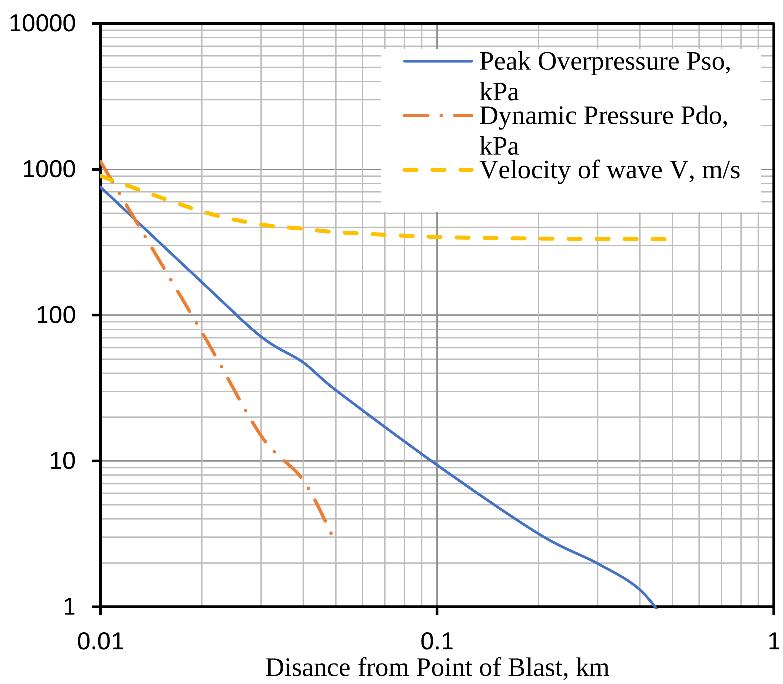

Figure 4. Variation of Pso, Pdo and shock front velocity with distance for 10kN weapon

2.2 Velocity of Shock Wave

Velocity of the shock wave is obtained by the expression:

$$V = V_0 \left[1 + \frac{6P_{so}}{7P_o}\right]^{0.5} \tag{3}$$

Where V_o is the velocity of sound in m/s (331 m/s), P_{so} is the peak overpressure in kPa and P_o is the atmospheric pressure, (101.325 kPa)

2.3 Reflected pressure

When a shock wave front impinges on the structure placed at the right angle of the direction of propagation of the wave, a reflection of shock front happens which is inexact twice the peak overpressure.
The reflected pressure acting on the structural surface is calculated using equation 3.

$$P_e = 2P_{s0}\,\frac{7P_0 + 4\,P_{s0}}{7P_0 + P_{s0}} \tag{4}$$

Where P_{so} is the peak overpressure, kPa, and P_o is the atmospheric pressure, kPa

Biggs (1964) [17] assumed that the effect of the reflected pressure depletes linearly, while it disappears to the sum of overpressure and dynamic pressure at a clearance time of t_c shown in Figure 5.

$$t_c = \frac{3S}{V} \tag{5}$$

Where S is half of the width of the structure or its height, least of the two.

V is the velocity of the shock front, m/s.

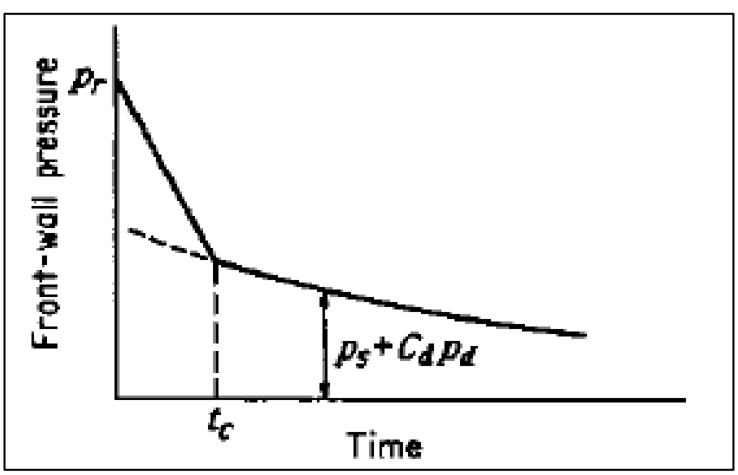

Figure 5. Variation of Reflected Pressure v/s time (Biggs,1964)

3. Model description

A 30-storey structure with peripheral shear wall and RC frame structure with central shear wall were modelled and analysed with 10 kN weapon blast load using ETABS. The dimension of the building structure was 25.00m× 25.00m in X and Y direction with 3.50m height from floor. The total height of the building for the 30-storeys was 105.00m. The building consists of a combination of structural elements such as columns, beams, slabs, and shear walls. Columns are the vertical components of the structure with the concrete grade of M40. The lower parts of the structure comprised of columns of larger cross-sectional areas and the sizes were reduced to a minimum in the higher storeys. The beams in the structure were horizontal components with a grade of M30. A rectangular section of the beam was used in the structure. The steel reinforcements in the column and beam sections were of grade Fe 500. Slab floor systems of grade M40 had a uniform thickness of 125mm. Slabs modelled as two-way slab systems using the shell-thin option in the tool. Shear walls were the vertical components with a M40 grade and had a thickness of 300mm. This covered the outer region and the core region. Tables 1 and 2 presents more details about the model's description and material properties. Three types of structures were modelled using the same structural details of this building, however, they differ on the outer face of the building as listed below.

3.1 Shear wall structure

A Closed RC frame structure is a regular building system with shear walls on the outer periphery. The plan and overall view of the building are depicted in the Figure 6. The outer concrete wall has the same properties of the concrete wall in the center of the building. This concrete wall system has no openings on the outer region, making it a shear wall structure.

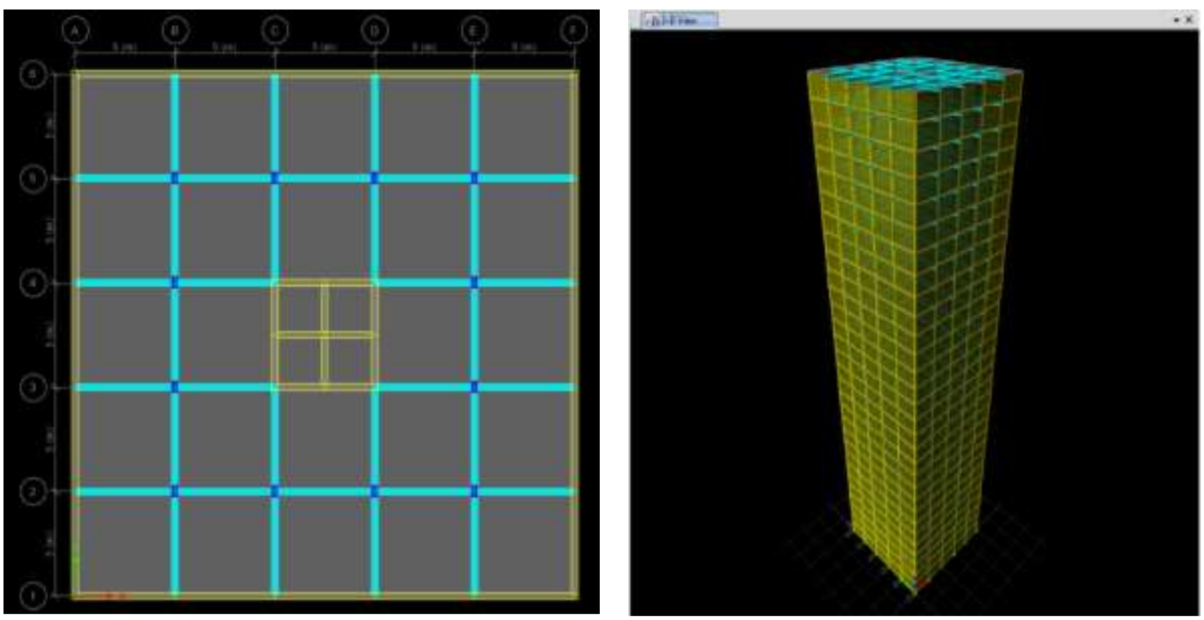

(a)2-D plane view (b)3D-plane view

Figure 6. View of RC shear wall structure

3.2 RC frame structure

The building is similar to Closed RC structure. However, shear walls are only available at the central region of the building. Figure 7 shows the floor plan and the three-dimensional view of the building

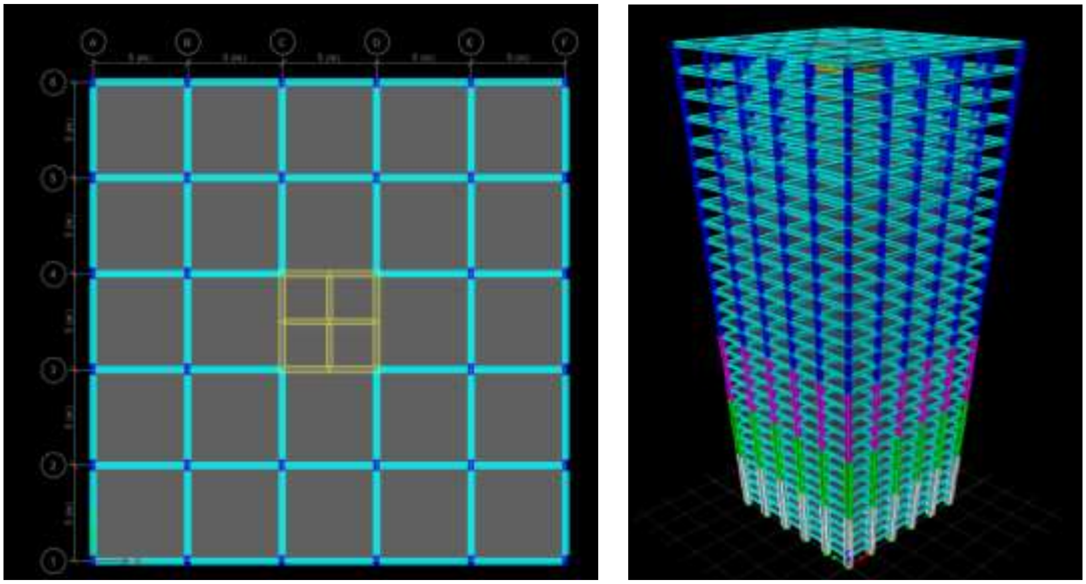

(a) 2-D plane view (b) 3D-plane view

Figure 7. View of RC frame structure

3.3 Masonry structure

A masonry structure is a regular building system that is almost the same as an RC frame structure but different as it has brick infill walls on the outer periphery. The plan and overall view of the building are depicted in the Figure 8.

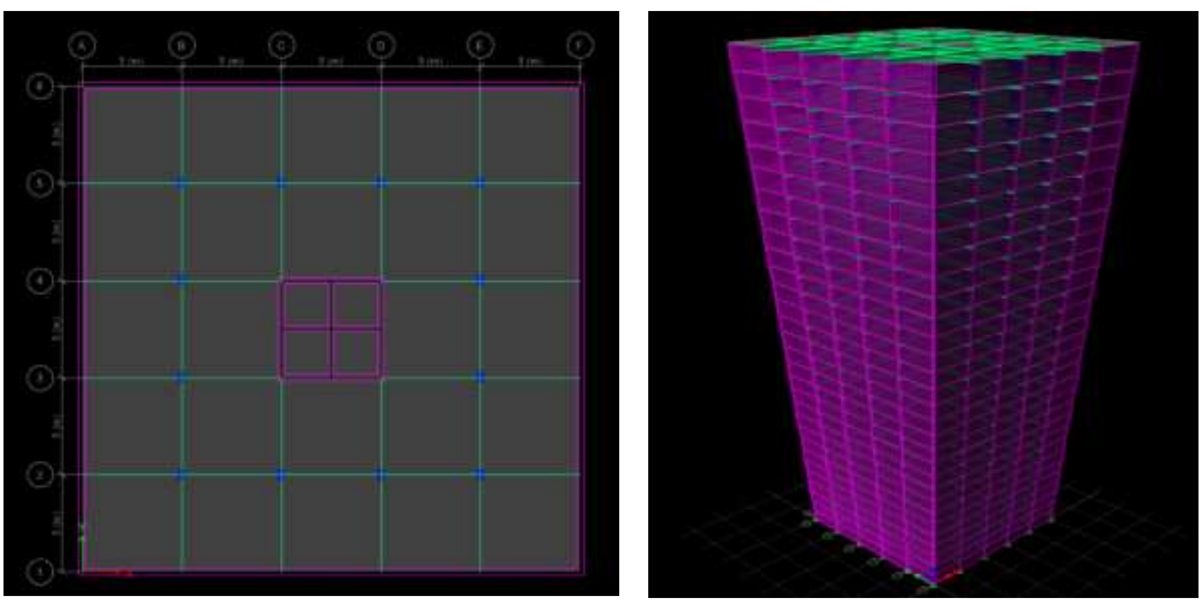

(a)2-D plane view (b)3D-plane view

Figure 8. view of the masonry structure

The three types of mentioned structures were modelled and analysed by subjecting it to a blast loading at stand-off distances of 0.050km, 0.070km, 0.090km, 0.110km and 0.150km.

Table 1 Model Description

Number of bays in x-direction		5	
Number of bays in y-direction		5	
Width of single bay in both the directions		5.00 m	
Number of Storeys		30	
Height of each storey		3.5 m	
Structural Elements	Column	800 mm x 800 mm from 0 - 5 storeys	M40
		600 mm x 600 mm from 5 - 10 storeys	
		500 mm x 500 mm from 10 - 15 storeys	
		300 mm x 300 mm from 15 - 30 Storeys	
	Beam	300mm x 600mm	M30
	Slab	125 mm thick	
	Shear wall	300 mm thick	M40

Table 2 Material properties

Structural Details	
Concrete, f_{ck}	M40
Steel, f_{st}	Fe500
Young's Modulus of M40 concrete, *E*	31622.77 MPa
Young's Modulus of steel, E_{st}	$2x10^5$ MPa
Density of concrete	25 kN/m^3
Density of steel	78.5 kN/m^3
Poisson's ratio, U	0.2

4. General loading

All types of structures had the same loading.The loadings applied to the building systems were according to the code IS 875-1987 part 2. Table 3 shows the general loadings on the structure. A load of infill was calculated as uniformly distributed load and applied on the beams. All three types of structures were located at zone II region and analysis of earthquake load was done according to the code IS 1893-2002. Design check was carried out to determine the adequacy of the system. The basic idea of this analogy is to study the response of a structure that is sound enough to resist the general gravity and seismic forces subjected to high impulse loads; in this case, a blast loading.

Table 3 load detailing applied in the structure

SL. No.	Type of Loads	Floor	Details
1	Live Load	Typical floor	3 kN/m^2
		Terrace Floor	1.5 kN/m^2
2	Floor finish	Typical floor	1 kN/m^2
		Terrace Floor	0.7 kN/m^2
3	Wall load	Floor beams	12.0 kN/m

5. Element details

Table 4 shows details of finite elements in the model. Each storey is assumed to have one Degree of Freedom (DOF). Therefore, the total DOF for a 30-storey building is 30 for all the three structures (RC shear wall, RC frame and masonry structures).

Table 4 Element details of the model

	Shear wall structure	RC Frame Structure	Masonry wall structure
Nodes	1271	1271	1271
Frames	1440	2640	1440
Shells	1684	1084	1684

6. Application of blast load

The structures were designed to resist seismic loading, after which, it is subjected to blast loading at various distances. The blast loading in ETABS is defined as a load-time triangular function within the model. As the stand-off distance is considered as a very important factor to determine the blast load parameters such as the velocity of sound, overpressure, and etc. The maximum distance between the blast source and the target were also documented to figure out where the effect of the blast will be reduced to the lowest range and fall in the underpressure zone.

A blast loading was created from a weapon charge of 10 kN and assigned at six different stand-off distances of 0.050km, 0.070km, 0.090km, 0.110km and 0.150km. A load-time triangular function was applied to the overall structure. As tabled in Table 5, the variety of overpressure and duration at various stand-off distances are presented.

Figures 9 and 10 were used to obtain the values of overpressure and duration of the 10 kN weapon to be used at various stand-off distances. The blast pressure loading was assumed to act per unit area of the structural element. Therefore, the pressure is multiplied with the unit area to calculate the blast loading for each particular stand-off distance. The obtained blast load was then applied as a point load at only one side of the structure.

Table 5 Variation of overpressure at different Stand-off distances for 10 kN weapon charge

Stand-off Distance, km	Overpressure, kPa	Duration, s
0.05	31	3.28
0.07	18	3.7
0.09	11	4.1
0.11	8	4.35
0.15	5	4.72

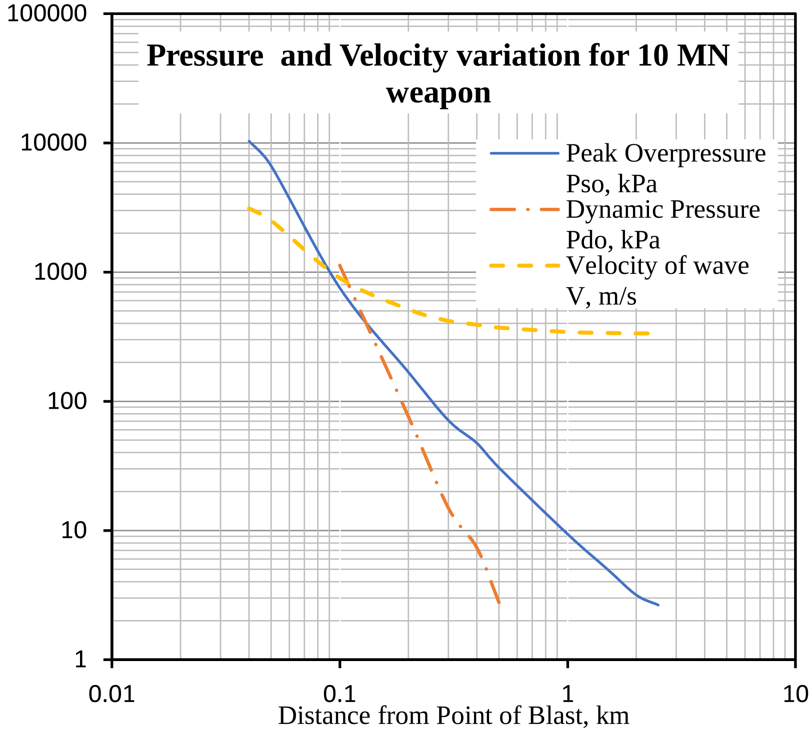

Figure 9. Variation of Overpressure, Dynamic Pressure and shock front velocity with distance for 10 kN weapon

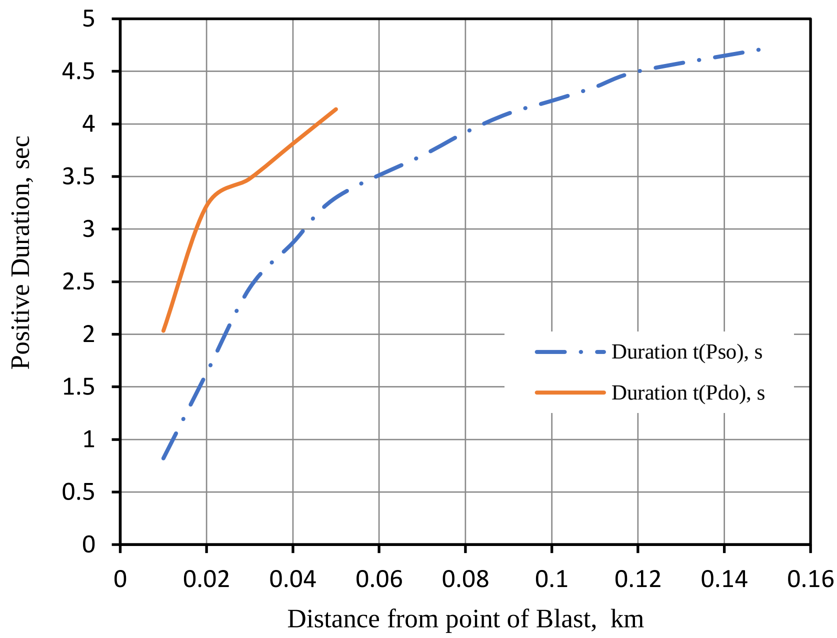

Figure 10. Variation of Duration of positive phase of Overpressure and Dynamic Pressure with distance for 10 kN weapon.

7. Analysis

A Single Degree of Freedom (SDOF) system was developed using analysis tools. The time period of the SDOF system was calculated. The blast load was defined as a triangular time history function in the ETABS. Hinges were assigned to beams and columns. Nonlinear analysis was considered due to material and geometry. Hilber-Hughes-Taylor (HHT) time integration method with the default values for alpha, beta and gamma were used. The step size was taken for each 0.01 seconds. A non-linear time history direct integration analysis was carried out.

8. Results

The behaviour of the building for the applied load was obtained from the numerical investigation. The obtained results of the analysis are listed below.

7.1 Von Mises Stress

The maximum Von Mises stress developed in all types of structures with the examined stand-off distances are tabulated in Table 6 below.

Table 6 Variations of stress with respect to the standoff distance, MPa

Standoff distance, km	Shear Wall Structure	RC Frame Structure	Masonry Wall Structure
0.050	106.13	84.44	90.05
0.070	35.43	72.35	55.43
0.090	12.98	25.65	31.39
0.110	6.89	10.89	6.03
0.150	2.68	8.90	2.36

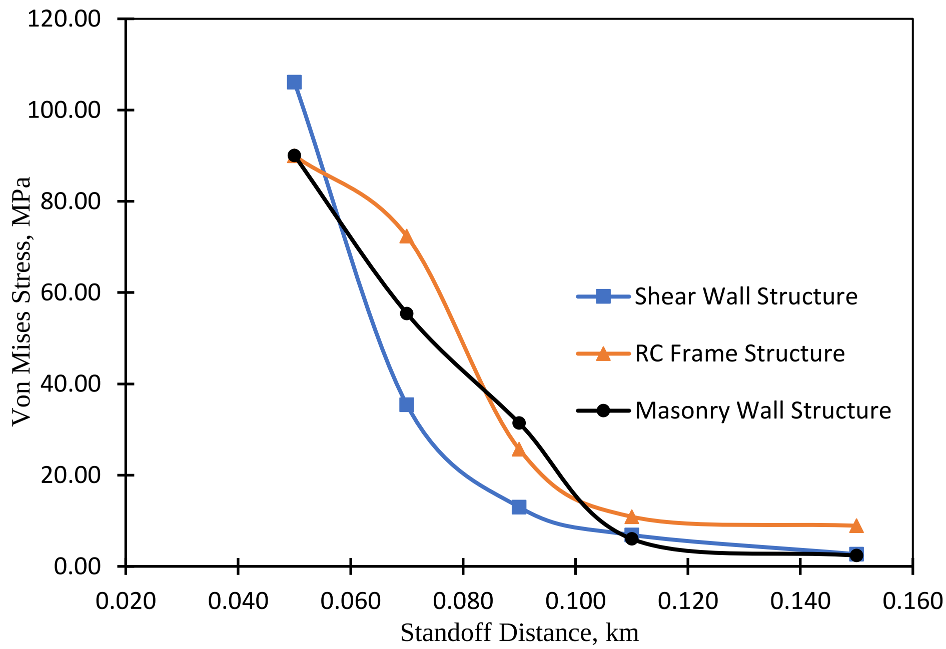

Figure 11. Maximum von mises stress, MPa at different standoff distance

From Figure 11 and Table 6, it is observable that, as the stand-off distance or the critical distance increases, the stress values on the wall elements reduces. At 0.050km the stress generated in the shear wall frame structure was 106.13 MPa and at 0.150km the stress generated was 2.68 MPa. Similarly, the stress in the RC frame structure at 0.050km was 84.44 MPa and at 0.150km it was 8.90 MPa. In the case of the masonry wall frame structure, the stress at 0.050km was 90.05 MPa and at 0.150km was 2.36 MPa. Taking this into consideration, the minimum or critical distance for a closed structure is found to be at 0.070km and 0.090km for both the RC frame structure and the Masonry Structure.

7.2 Top storey acceleration

Table 7 shows the variations of the acceleration of a particular joint at the top storey in all the three studied structures. The variation of the acceleration with respect to stand-off distance is inversely proportional. As the distance increases, the acceleration of a particular joint decreases in all the three cases studied. While Figure 8 represents the variation of the top storey acceleration with respect to the critical or stand-off distance in shear wall structure, RC frame structure and masonry wall structure respectively.

Table 7 Top Storey Acceleration, mm/sec^2

Standoff distance, km	Shear wall structure	RC Frame Structure	Masonry Wall Structure
0.05	9570.91	7761.51	5285.95
0.07	3246.49	4320.2	3246.49
0.09	1216.38	2015.91	666.4
0.11	644.48	1064.19	352.58
0.15	393.24	417.13	137.77

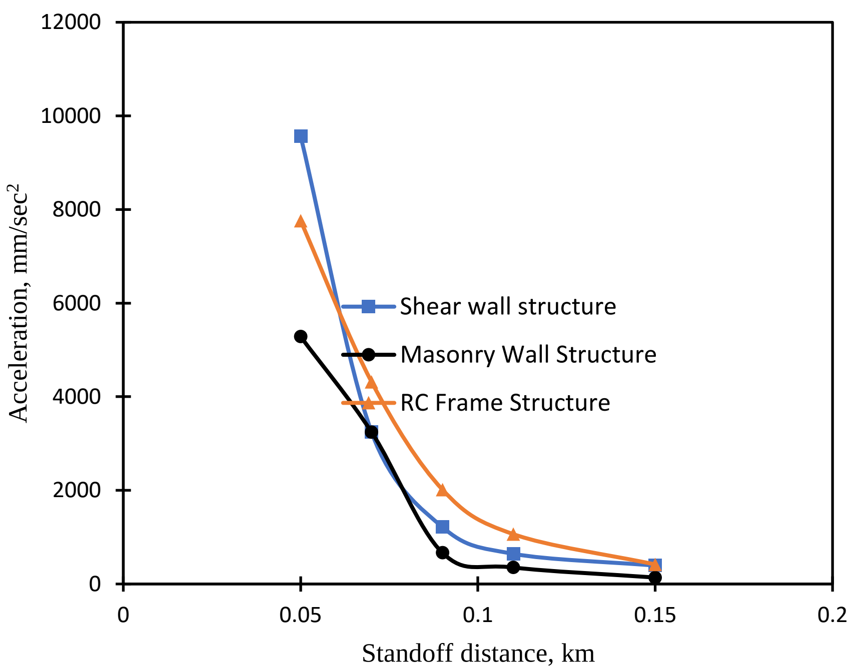

Figure 12. Top storey acceleration of Shear Wall, RC frame and masonry structures wall structure

From the above Table 7 and Figure 12, we can conclude that the stand-off distance plays an important role in the case of the response to acceleration of the building subjected to the blast pressure.

8.3 Top Storey Displacement

A study on the displacement parameter for all the models at different stand-off distances and top storey displacement values are tabulated below. Table 8 shows the variations of the displacement of a particular joint at the top storey in all three types of structures. From the table we can conclude that the stand-off distance plays an important role in the case of the response of the building subjected to blast pressure.

Table 8 Top Storey Displacement, mm

Standoff distance, km	Shear wall structure	RC Frame Structure	Masonry Wall Structure
0.05	548.13	477.28	400
0.07	185.57	404.74	185.57
0.09	69.8	300	75.36
0.11	37.09	230.98	23.22
0.15	14.76	92.1	8.99

Figure 13 represents the variation of the top storey displacement with respect to the critical or stand-off distance in the shear wall structure, RC frame structure and masonry wall structure, respectively.

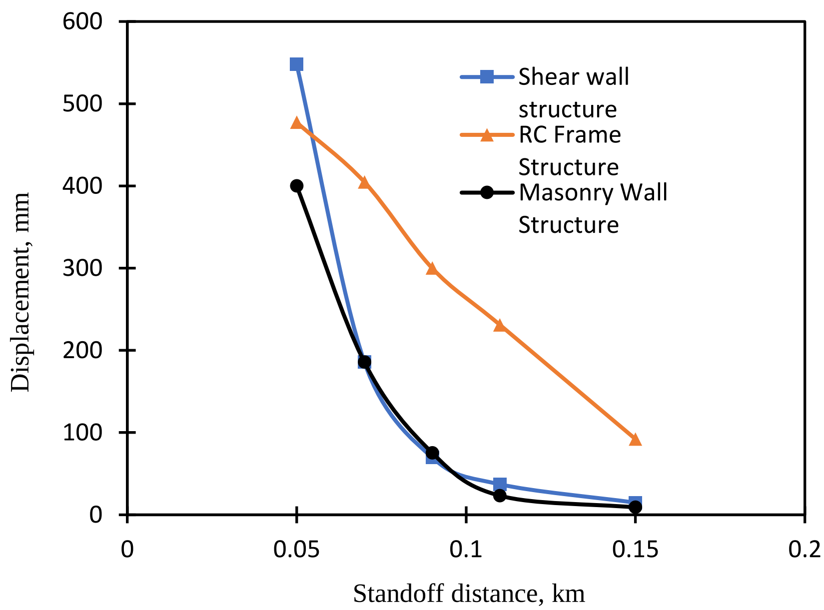

Figure 13. Top Storey Displacement of Shear Wall, RC frame and masonry structures

From the obtained results, the variation of displacement with respect to stand-off distance is inversely proportional. As the distance increases, the displacement of a particular joint decreases in all three cases in the study.

8.4 Maximum story displacement

The maximum storey displacement of shear wall, RC frame and masonry wall structures were recorded at the critical stand-off distance of 0.090km with 10 kN weapon charge. The maximum displacement of the building with the variation of storeys are presented in Table 9 and Figure 14

Table 9 Maximum displacement in each storey, mm

Story	Elevation, m	Shear Wall Structure	RC frame	Masonry structure
30	105	10.259	4.525	0.518
29	101.5	10.142	4.386	0.499
28	98	10.041	4.257	0.479
27	94.5	9.955	4.141	0.459
26	91	9.883	4.044	0.439
25	87.5	9.824	3.972	0.418
24	84	9.777	3.922	0.398
23	80.5	9.733	3.892	0.377
22	77	9.689	3.881	0.356
21	73.5	9.637	3.888	0.335
20	70	9.57	3.905	0.315
19	66.5	9.479	3.92	0.294
18	63	9.35	3.923	0.273
17	59.5	9.173	3.911	0.253
16	56	8.94	3.886	0.232
15	52.5	8.646	3.852	0.212
14	49	8.293	3.817	0.193
13	45.5	7.884	3.792	0.173
12	42	7.427	3.787	0.155
11	38.5	6.926	3.807	0.136
10	35	6.383	3.842	0.119
9	31.5	5.799	3.858	0.102
8	28	5.175	3.809	0.086
7	24.5	4.516	3.641	0.071
6	21	3.832	3.333	0.056
5	17.5	3.136	2.884	0.043
4	14	2.436	2.318	0.031
3	10.5	1.743	1.658	0.021
2	7	1.079	0.978	0.012
1	3.5	0.475	0.372	0.005

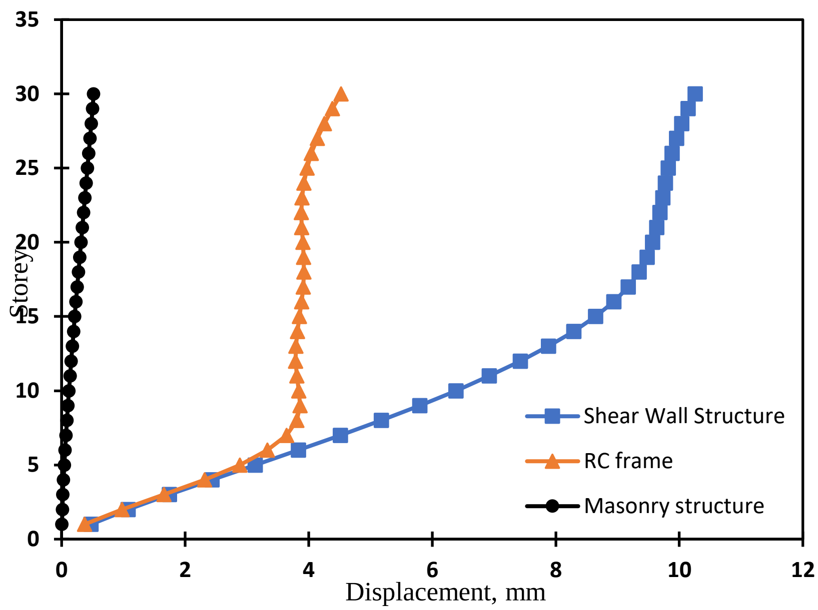

Figure 14. Maximum displaceemnt in each storey at critical distance

9. Maximum storey drift

the maximum storey drift of the RC shear wall, RC frame and masonry structures were obtained with a critical distance of 0.090 km with 10 kN weapon charge. Table 10 and Figure 13 present the maximum drift of variation in each storey of the building.

Table 7.10 Maximum drift in each storey

Story	Shear Wall Structure	RC frame	Masonry structure
30	0.001952	0.000631	0.000006
29	0.001971	0.000637	0.000006
28	0.001992	0.000654	0.000006
27	0.002012	0.000683	0.000006
26	0.002031	0.000726	0.000006
25	0.002045	0.000783	0.000006
24	0.002056	0.000851	0.000006
23	0.002062	0.00093	0.000006
22	0.002064	0.001017	0.000006
21	0.002062	0.001108	0.000006
20	0.002056	0.001201	0.000006
19	0.002046	0.001299	0.000006
18	0.002031	0.001401	0.000006
17	0.002012	0.001505	0.000006
16	0.001986	0.00161	0.000006
15	0.001952	0.001697	0.000006
14	0.001911	0.001818	0.000006
13	0.001862	0.001954	0.000005
12	0.001806	0.002095	0.000005
11	0.001741	0.002241	0.000005

10	0.001668	0.002348	0.000005
9	0.001586	0.002463	0.000005
8	0.001495	0.002546	0.000004
7	0.001393	0.002602	0.000004
6	0.00128	0.002634	0.000004
5	0.001155	0.002613	0.000003
4	0.001017	0.002579	0.000003
3	0.000864	0.002508	0.000003
2	0.000697	0.002363	0.000002
1	0.000443	0.001181	0.000001

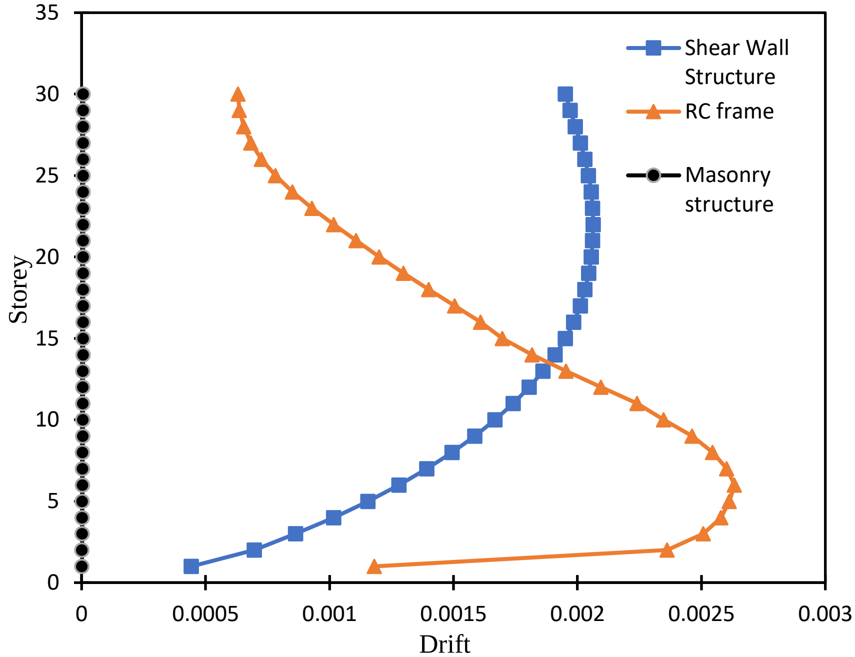

Figure 15. Maximum storey drift at critical distance

10. Conclusion

This work presents the dynamic response of three types of structures when subjected to blast loads of a particular weapon charge. Parameters such as varying overpressure that functions at a stand-off distance were applied to the systems and to determine the critical distances of blast load effects. A 30-storey structure was used as a model for this study. All the models were analysed using the software package ETABS. This study was carried out to examine the behaviour of the structures at varying distances of explosion from the source of the blast. Von Mises stress considered the important factors that help in determining the stability of a structure. From the design, the failures occurred in a structure when the obtained Von Mises stress reached the maximum value. Meanwhile, its reach is a value greater than the strength of the materials in the structures. From the obtained results, the RC shear wall records that the maximum Von Mises stresses were developed at approximately 1.5 to 2 times more than the stresses obtained from the opened RC frame. Also, it can be concluded that as the stand-off distance or the critical distance increases, the stress values on the wall element reduces. The Von Mises stresses developed on the outer walls of the structures at a distance of 0.050km was 106.13 MPa, which was greater than the concrete strength which was M40. At this stress value, the structure collapsed. In addition, it was also recorded that at 0.150km, the stress value was 2.86 MPa. Similarly, the stress in RC frame structure at 0.050km was 84.44 MPa and at 0.150km was 8.90 MPa. While in the masonry wall frame structure, the stress recorded at 0.050km was 90.05 MPa. Therefore, the minimum safe distance is 0.070km for shear wall structure and 0.090km for both the RC frame and masonry wall structures. The other responses of the storey displacement and storey drift were also obtained for the RC shear wall, RC frame and masonry structures at their respective stand-off distances.

REFERENCES

[1] D. A. Crowl, *Understanding explosions*, vol. 16. John Wiley & Sons, 2010.
[2] S. Glasstone, *The effects of nuclear weapons*. US Atomic Energy Commission, 1962.
[3] N. Khatavakar, B. Raghu Prasad, and K. Amarnath, “Response of High Rise Structures Subjected To Blast Loads,” *Int. J. Sci. Eng. Technol. Res. Vol.*, vol. 5, 2016.
[4] A. A. Kore and N. P. Phadtare, “A Review on ‘Analysis, design and study of behavior of RC Structure under Blast loading of various intensities,’” 2018.
[5] G. Mays, P. D. Smith, and P. D. Smith, *Blast effects on buildings: Design of buildings to optimize resistance to blast loading*. Thomas Telford, 1995.
[6] J. Li, C. Wu, and H. Hao, “An experimental and numerical study of reinforced ultra-high performance concrete slabs under blast loads,” *Mater. Des.*, vol. 82, pp. 64–76, 2015.
[7] I. G. Cullis, “Blast waves and how they interact with structures,” *J. R. Army Med. Corps*, vol. 147, no. 1, pp. 16–26, 2001.
[8] C. A. Handley, B. D. Lambourn, N. J. Whitworth, H. R. James, and W. J. Belfield, “Understanding the shock and detonation response of high explosives at the continuum and meso scales,” *Appl. Phys. Rev.*, vol. 5, no. 1, p. 11303, 2018.
[9] C. Zhang, B. Huang, Z. Luo, X. Che, P. Yan, and T. Shao, “Atmospheric-pressure pulsed plasma actuators for flow control: shock wave and vortex characteristics,” *Plasma sources Sci. Technol.*, vol. 28, no. 6, p. 64001, 2019.
[10] N. Artemieva and V. Shuvalov, “Atmospheric shock waves after impacts of cosmic bodies up to 1000 m in diameter,” *Meteorit. Planet. Sci.*, vol. 54, no. 3, pp. 592–608, 2019.
[11] H. L. Brode, “A review of nuclear explosion phenomena pertinent to protective construction,” RAND CORP SANTA MONICA CA, 1964.
[12] M. Neff and E. Fiume, “A visual model for blast waves and fracture,” in *Graphics Interface*, 1999, vol. 99, pp. 193–202.
[13] D. Gabel, “Explosion Process Safety: Basics and Application of Explosion Protection,” in *Safety and Security Issues in Technical Infrastructures*, IGI Global, 2020, pp. 203–231.
[14] D. Y. Akimov *et al.*, “Coherent elastic neutrino scattering on atomic nucleus: recently discovered type of low-energy neutrino interaction,” *Physics-Uspekhi*, vol. 62, no. 2, p. 166, 2019.
[15] F. Masi, I. Stefanou, P. Vannucci, and V. Maffi-Berthier, “Resistance of museum artefacts against blast loading,” *J. Cult. Herit.*, 2020.
[16] J. Lee, T. E. Lacy Jr, C. U. Pittman Jr, and J. N. Reddy, “Numerical estimations of lightning-induced mechanical damage in carbon/epoxy composites using shock wave overpressure and equivalent air blast overpressure,” *Compos. Struct.*, vol. 224, p. 111039, 2019.
[17] Biggs. J.M, “Introduction to Structural Dynamics”, McGraw-Hill, New York, 1964
[18] IS 4991.1968 - Criteria for blast resistant design of structures for explosions above ground